

Ultrafast Mott transition driven by nonlinear phonons

Francesco Grandi,¹ Jiajun Li,¹ and Martin Eckstein¹

¹*Department of Physics, University of Erlangen-Nürnberg, 91058 Erlangen, Germany*

(Dated: November 27, 2021)

Nonlinear phononics holds the promise for controlling properties of quantum materials on the ultrashort timescale. Using nonequilibrium dynamical mean-field theory, we solve a model for the description of organic solids, where correlated electrons couple non-linearly to a quantum phonon-mode. Unlike previous works, we exactly diagonalize the local phonon mode within the non-crossing approximation (NCA) to include the full phononic fluctuations. By exciting the local phonon in a broad range of frequencies near resonance with an ultrashort pulse, we show it is possible to induce a Mott insulator-to-metal phase transition. Conventional semiclassical calculations, where the quantum phonon operators are replaced by their classical expectation values, fail to capture the insulator-to-metal transition. This fact, together with the non-thermal character of the photo-induced metal, suggests a leading role of the phononic fluctuations and of the dynamic nature of the state in the vibrationally induced quasiparticle coherence.

Introduction - In the last decade, nonlinear phononics [1, 2] has become one of the most promising pathways for the non-equilibrium control of quantum materials [3]. Within this approach, one can transiently stabilize a crystal structure unstable under equilibrium conditions by coherently exciting an infrared-active lattice mode which is nonlinearly coupled to a Raman-active phonon [4–10]. An analogous pathway suggests that the electronic properties of solids may be manipulated by the excitation of vibrational modes that couple non-linearly with the local parameters of the electronic system [11–15].

Molecular solids provide a perfect playground for testing this mechanism [16, 17]. A paradigm example is the charge transfer salt ET-F₂TCNQ, which is an archetypical one-dimensional Mott insulator under equilibrium conditions and has been widely studied under photo-doping [18, 19]. Upon excitation of the molecular vibration $\omega_{\text{ph}} = 1000 \text{ cm}^{-1}$, the charge transfer (CT) resonance at $\sim 5500 \text{ cm}^{-1}$ is red-shifted, and an in-gap state at $2 \times \hbar\omega_{\text{ph}}$ appears [11, 20]. Even more intriguing results have been obtained regarding light-induced superconductivity. The fulleride K₃C₆₀ [21] shows a superconducting state at temperatures almost ten-times higher than the equilibrium T_c lasting few-picoseconds after excitation in the frequency range related to the T_{1u} mode of the C₆₀ molecule [22–24]. The organic superconductor κ -(BEDT-TTF)₂Cu[N(CN)₂]Br (henceforth κ -Br) displays a similar behavior when the C=C stretching mode of the (BEDT-TTF)^{+0.5} molecule is excited [25]. Because the photo-induced superconducting response is correlated with the presence of an equilibrium coherent quasiparticle, it is an obvious relevant question, which will be analyzed in this paper, whether non-linear phonics can enhance quasiparticle coherence in correlated electron systems.

One often analyzes nonlinear phononics starting from a semiclassical approximation for the driven vibrational mode. A typical rather local electron-phonon interaction gO_iX_i , where an electronic operator O_i couples to the displacement X_i of atom i , would give a term $F_i(t)O_i$ with a time-dependent “force” $F_i(t) = g\langle X_i(t) \rangle$

in the electronic Hamiltonian when X_i is replaced by its time-dependent expectation value in a coherent (macroscopically occupied) $\mathbf{q} = 0$ phonon state. For example, the experiments on ET-F₂TCNQ and κ -Br were interpreted by an average shift and a periodic time-dependence of the local Coulomb interaction (the Hubbard U) [11, 25, 26]. However, it is clear that the approximation $O_iX_i \approx O_i\langle X_i(t) \rangle$ is controlled by the fluctuations of the local displacement operator X_i relative to $\langle X_i(t) \rangle$, which are significant even when the phonons are globally in a macroscopic coherent mode. Even though the semiclassical analysis can successfully capture some experimental observations, it is, therefore, important to understand how quantum effects become manifest in nonlinear electron-phononics [20].

In this paper, we study a generalization of the dynamic Hubbard model [27, 28], which applies to ET-F₂TCNQ and κ -Br, with a quadratic coupling of a local displacement X_i to the doublon and the holon densities, so that, on average X_i^2 modulates a local electron interaction U . The simulations indeed predict an insulator-to-metal transition (IMT), with a strong enhancement of the quasiparticle weight driven by the excitation of the local vibration. The vibrationally induced metallicity in the model cannot be accounted for by a semiclassical Hamiltonian in which a time-dependent U replaces the effect of the phonons, but instead the full quantum dynamics must be taken into account. Moreover, the semiclassical model also lacks the back-action of electrons on the phonons and cannot capture phonon-related features in the electronic spectrum (Fano resonances) [29, 30].

Model - We consider the generalized dynamic Hubbard model, compactly written as:

$$H(t) = H_{\text{el}} + H_{\text{el-ph}} + H_{\text{ph}} + H_{\text{driv}}(t) - \mu N. \quad (1)$$

The purely electronic part of the Hamiltonian is given by

$$H_{\text{el}} = -v_0 \sum_{\langle i,j \rangle, \sigma} \left(c_{i,\sigma}^\dagger c_{j,\sigma} + \text{H. c.} \right) + U \sum_i n_{i,\uparrow} n_{i,\downarrow}, \quad (2)$$

with nearest-neighbor hopping v_0 and local Hubbard interaction U ; μ is the chemical potential used to fix the

occupation of each site to $\langle n_i \rangle = 1$. $v_0 = 1$ and \hbar/v_0 set the units for the energy and the times, respectively. The bare phonon Hamiltonian in Eq. (1) describes a band of Einstein phonons $H_{\text{ph}} = \omega_{\text{ph}} \sum_i (a_i^\dagger a_i + \frac{1}{2})$ where a_i^\dagger (a_i) are the creation (destruction) operator for a boson.

The electron-phonon interaction is given by [20]:

$$H_{\text{el-ph}} = 2 \sum_i (h H_i - d D_i) X_i^2, \quad (3)$$

where $H_i = (1 - n_{i,\uparrow})(1 - n_{i,\downarrow})$ ($D_i = n_{i,\uparrow}n_{i,\downarrow}$) are the holon (doublon) operators, and $X_i = \frac{a_i^\dagger + a_i}{\sqrt{2}}$ is the local displacement. We take parameters $\omega_{\text{ph}} = 1.5$, and assume the values $h = 0.1$ and $d = 0.35$ for the coupling constants. With this, the renormalized phonon frequencies on an isolated site occupied by a holon or doublons are $\omega_{\text{ph}}^h \sim 1.24 \omega_{\text{ph}}$ and $\omega_{\text{ph}}^d \sim 0.26 \omega_{\text{ph}}$, respectively, in agreement with the parameters for ET-F₂TCNQ [20]. Note that $H_{\text{el-ph}}$ with $d \neq h$ breaks the particle-hole symmetry even on a bipartite lattice [31]. In experiments, the quadratic coupling of the phonon-displacement and the electrons is confirmed by the $2\omega_{\text{ph}}$ feature in the optical absorption after phonon excitation [20]. The last term in Eq. (1) describes a linear coupling of the phonon displacement to an external electric field,

$$H_{\text{driv}}(t) = \sqrt{2}\omega_{\text{ph}} f(t) \sum_i X_i, \quad (4)$$

and we use a few-cycle excitation pulse $f(t)$ with different frequencies Ω (see Fig. 1 inset) to excite a coherent vibration of the phonon. Finally, we will compare the dynamics obtained from Eq. (1) with a semiclassical approximation, in which the electron dynamics is determined by Eq. (2) with a time-dependent interaction U

$$H_{\text{U-driv}}(t) = H_{\text{el}}[U \rightarrow U(t)], \quad (5)$$

with different forms of $U(t)$ as described in the text.

We solve the time-dependent models Eq. (1) and Eq. (5) using non-equilibrium dynamical mean-field theory (NEDMFT) within non-crossing approximation (NCA) [32, 33]. NEDMFT maps the lattice problem into an Anderson impurity model with a self-consistent hybridization function $\Delta(t, t')$. We use a semi-elliptic free density of states of width $4v_0$, leading to the closed form $\Delta(t, t') = v_0^2 G(t, t')$ in terms of the local contour-ordered electronic Green's function $G(t, t')$. For model (1), we include the full phonon Fock space and the nonlinear local electron-phonon dynamics exactly in the DMFT impurity model (similar to bosonic DMFT [34]) and take the cut-off in the phonon Hilbert space large enough ($N_{\text{ph}} = 18$ for mean occupations $|\langle X \rangle| \lesssim 1$). This avoids potential ambiguities of alternative diagrammatic approaches for the local electron-phonon interaction [35–37]. Details of the implementation will be published elsewhere.

Finally, energy dissipation of electrons to other degrees of freedom (phonons, spin fluctuations, etc.), which is fast in correlated insulators, is taken into account through a

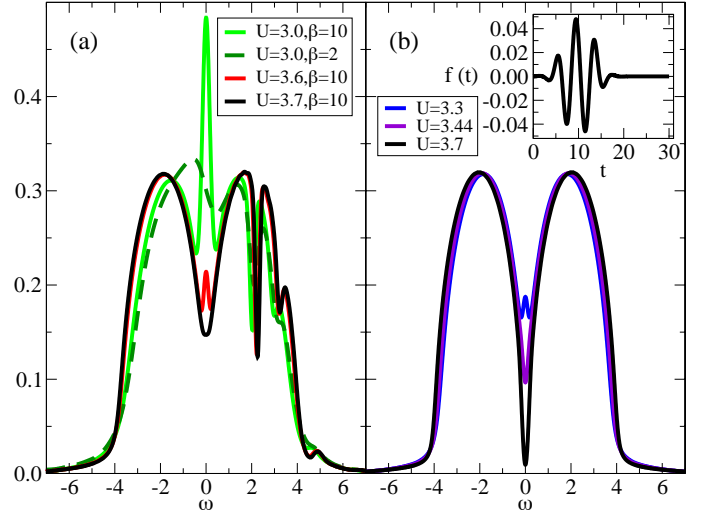


Figure 1. (Color online) (a) Equilibrium spectral functions $A(\omega)$ for the electron-phonon coupled system at several values of U and inverse temperature β . (b) Same for the Hubbard model without dynamic phonons, at $\beta = 10$. Inset: time dependent driving field $f(t)$, cf. Eq. (4). We keep the maximum amplitude (0.05) and the duration (20), while the frequency Ω is changed ($\Omega = 1.5$ in the plot, equal to ω_{ph}).

bosonic heat bath. The bath just adds a term to the hybridization [38, 39], $\Delta(t, t') = v_0^2 G(t, t') + \Delta_{\text{Ohmic}}(t, t')$, where $\Delta_{\text{Ohmic}}(t, t') = \lambda G(t, t') D_{\text{Ohmic}}(t, t')$ is first order in the coupling of electrons to bosonic modes with temperature $1/\beta$ and Ohmic density of states (bath spectral density $J(\omega) = \sum_\alpha g_\alpha^2 \delta(\omega - \omega_\alpha) = \omega \theta(\omega_c - \omega)$, $\omega_c = 0.2$). We take $\lambda = 0.242$, which is weak enough so that electronic spectra are not affected by the coupling to the bath.

Results - In Fig. 1a, we plot the electronic spectral function $A(\omega)$ of the dynamic Hubbard model (1) for several values of the interaction U . At low temperature ($\beta = 10$), there is an IMT around $U = 3.6$, indicated by the appearance of a quasi-particle peak at $\omega \sim 0$. With increasing temperature, the quasi-particle peak vanishes, as the system crosses over into a bad metallic regime (see data for $U = 3.0$ and $\beta = 2$). The pronounced dip in the upper Hubbard band results from the interference between the electronic states and the phonon.

We now concentrate on parameters $U = 3.7$ and $\beta = 10$ above the IMT and attempt to induce the transition through phonon driving. The vibrational mode is pumped using a few-cycle pulse $f(t)$ as shown in the inset of Fig. 1, at different frequencies Ω . Figure 2 displays the resulting time-evolution of several observables. While $\langle X \rangle$ oscillates around its equilibrium position $\langle X \rangle = 0$ with the bare phonon frequency $\sim \omega_{\text{ph}}$ (Fig. 2a), $\langle X^2 \rangle$ oscillates around a shifted mean at a frequency $\sim 2\omega_{\text{ph}}$ (Fig. 2b). The most pronounced response is observed at resonant pumping $\Omega = \omega_{\text{ph}} = 1.5$. At resonance, the double occupancy increases by about 15% compared to its initial value (Fig. 2c). These changes go along with a

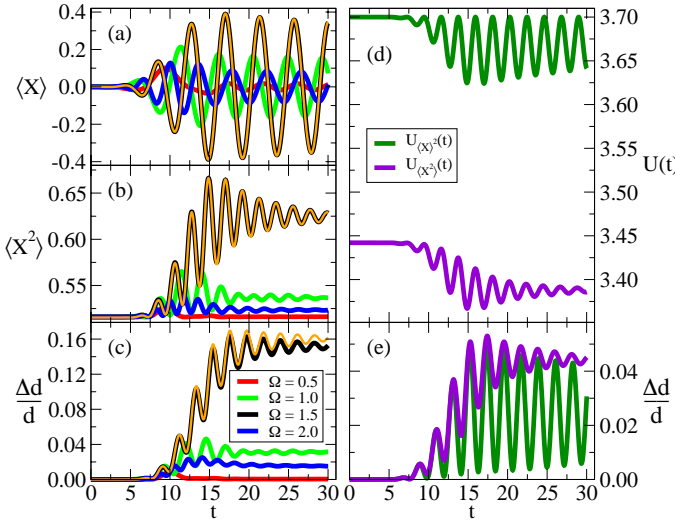


Figure 2. (Color online) Time evolution of the expectation value of the position operator $\langle X \rangle$ (a), its square $\langle X^2 \rangle$ (b), the relative change of the double occupations with respect to the initial value $\frac{\Delta d}{d} = \frac{d(t) - d(0)}{d(0)}$ (c), at $U = 3.7$, $\beta = 10$, and field pulses $f(t)$ of different frequencies Ω . The thin orange lines represent the results at $\Omega = 1.5$ without Ohmic bath. (d) Time dependent $U_{\langle X \rangle^2}(t)$, and $U_{\langle X^2 \rangle}(t)$, as defined in Eq. (6), where the expectation value $\langle X(t) \rangle$ ($\langle X^2(t) \rangle$) corresponds to the black line at $\Omega = 1.5$ of panel a (b). (e) Time-dependent $\frac{\Delta d}{d}$ as obtained from Eq. (5), with $U(t)$ shown in panel (d).

photo-induced metallicity, as observed from the transient appearance of a quasi-particle peak at $\omega \sim 0$ in the time-resolved spectral function (Fig. 4, upper panels). The metallization survives the switch-off of the laser pulse up to the latest time ($t = 30$) of the simulation (Fig. 4g). In addition to the quasi-particle peak, one observes oscillations at frequency $2\omega_{\text{ph}}$ in the spectrum, like in $\langle X^2 \rangle$. The broad range of frequencies Ω where we observe the onset of the peak at $\omega \sim 0$ verifies the genuine metallicity of the photo-induced state, with a small asymmetry around the observed maximum response, see Fig. 3.

We will now contrast these results with the semiclassical model Eq. (5), where phonon variables in the electron-phonon interaction Eq. (3) are replaced by a classical field, leading to a time-dependent interaction. We compare two possible ansatzes, where X_i^2 is replaced by either $\langle X(t) \rangle^2$, or by $\langle X^2(t) \rangle$. This substitution gives

$$U \rightarrow \begin{cases} U - 2(d-h)\langle X(t) \rangle^2 \equiv U_{\langle X \rangle^2}(t) \\ U - 2(d-h)\langle X^2(t) \rangle \equiv U_{\langle X^2 \rangle}(t) \end{cases}, \quad (6)$$

taking into account that $\sum_i H_i = \sum_i D_i$ up to terms $\propto \hat{N}$. In both cases, the DMFT solution of the full model provides the expectation value; Fig. 2d shows the resulting $U(t)$ for the almost-resonant driving case $\Omega = 1.5$. Clearly, for a general state of the quantum phonon, $\langle X \rangle^2 \neq \langle X^2 \rangle$. A time-dependent function of the kind $U(t) = U + \Delta U [1 - \cos(2\omega_{\text{ph}}t)] \theta(t)$ can qualitatively describe the U-driving guided by $\langle X \rangle$, while

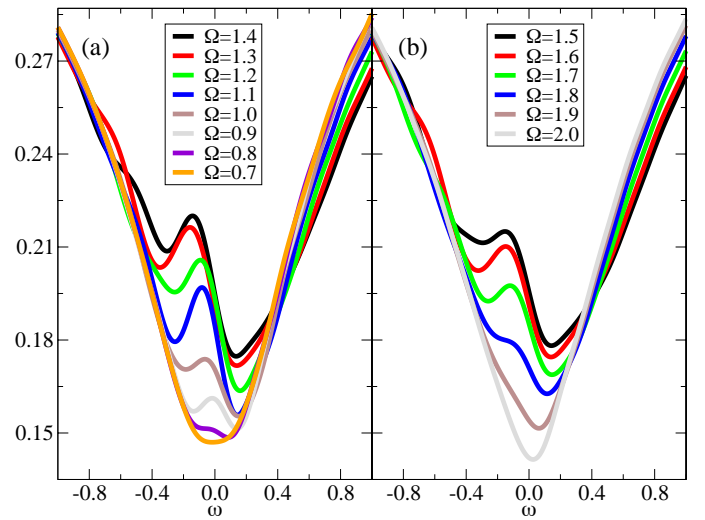


Figure 3. (Color online) Zoom around $\omega \sim 0$ of the time dependent (backward) spectral functions $A(\omega, t) = -\frac{1}{\pi} \text{Im} \int ds G^R(t, t-s) e^{i\omega s}$ at $t = 30$ after excitation pulses with frequency Ω below (a) and above (b) the bare phonon frequency ω_{ph} .

$U_{\langle X^2 \rangle}(t)$ looks more like an interaction quench.

We note that $U_{\langle X^2 \rangle} \neq U$ already in equilibrium, where the vacuum and thermal fluctuations of the phonon are responsible for a renormalization of U by ~ -0.3 . In equilibrium, one finds that this renormalization rather accurately accounts for the shift of the IMT in the dynamic Hubbard model as compared to the standard Hubbard model. In Fig. 1b, we show the equilibrium spectra of the Hubbard model at different U ; the IMT in the dynamic Hubbard model Eq. (1) is indeed lowered by ~ -0.3 compared to the static one. This quantitative agreement also shows that for the given parameters polaronic effects play a minor role in localizing the quasi-particles, at least under equilibrium conditions (clearly, the static Hubbard model cannot reproduce the phonon signatures in the upper Hubbard band). In contrast to this observation, the non-equilibrium dynamics of quasi-particles and the vibrationally induced IMT in the dynamic Hubbard model cannot be explained by a renormalized time-dependent interaction. We compare in Fig. 4 the time-dependent spectra $A(\omega, t)$ for the three analyzed cases. While we still notice some increase in the spectral weight at zero frequency, neither the quench-like $U(t) = U_{\langle X^2 \rangle}(t)$ (lower panels) nor the stronger time-periodic form $U(t) = U_{\langle X \rangle^2}(t)$ (middle panels) reproduce the emergence of a zero-frequency peak. The rather different response of the dynamic Hubbard model and the effective model is evident also in other observables: the relative change $\Delta d/d \sim 15\%$ in the double occupancy at resonant driving is almost three times larger than the change $\Delta d/d$ in the Hubbard model in response to the corresponding time-dependent interactions (cf. Figs. 2c and e).

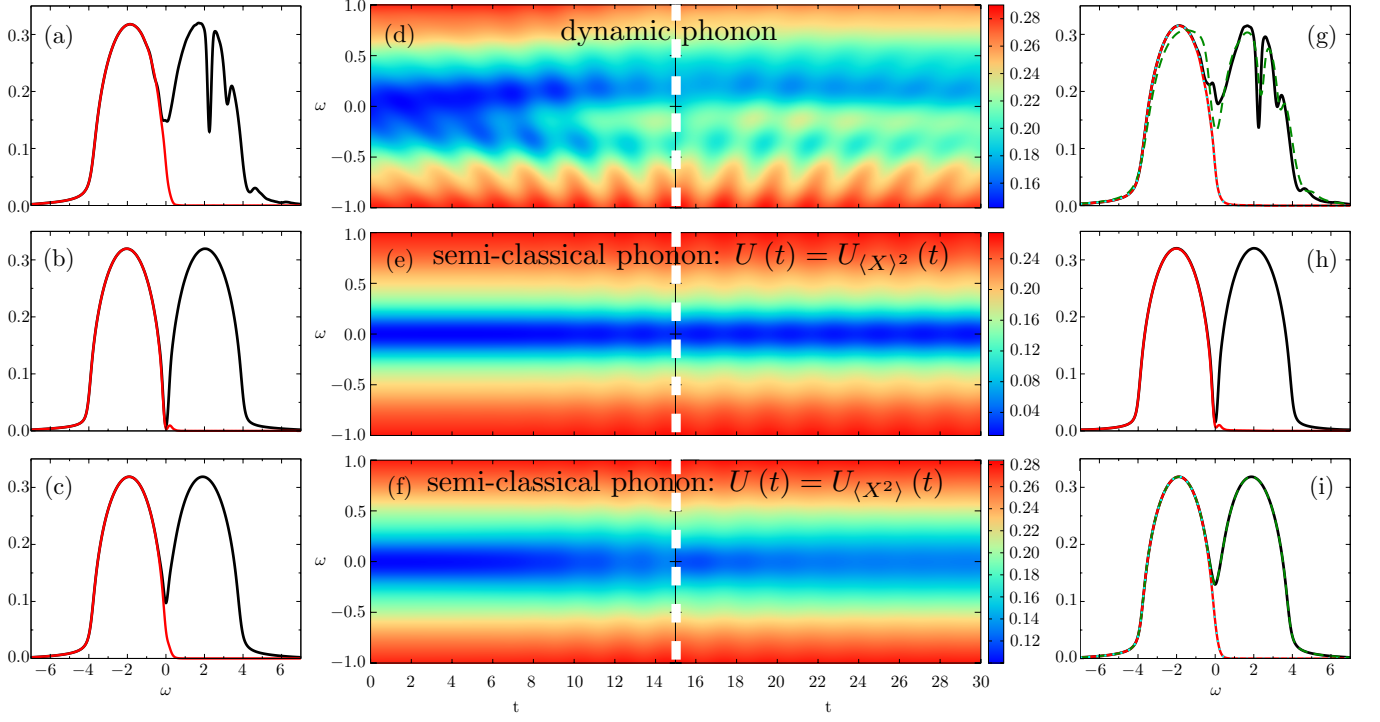


Figure 4. (Color online) Time-dependent spectral functions for the dynamic phonon model at $U = 3.7$ (upper row), the semiclassical model with $U(t) = U_{\langle X \rangle}^2(t)$ as shown in Fig. 2d (middle row), and $U(t) = U_{\langle X^2 \rangle}(t)$ (bottom row). Spectral function and occupation (black and red lines, respectively) at initial time $t = 0$ and at latest time $t = 30$ are shown in the left columns (a-c) and right columns (g-i), respectively. Additional lines in (g) and (i) show a fit $A^<(\omega, t) = A(\omega, t)/(1 + e^{\beta_{\text{eff}}\omega})$ to the occupation functions (dotted cyan lines), and the equilibrium spectral function (dashed green lines) for a system with the same total energy as the driven system at latest time $t = 30$ ($\beta \sim 2.083$ for the phonon case, $U \sim 3.388$ and $\beta = 10$ for the U -driven case). Middle panels (d-f): Time dependent spectral weight close to the Fermi level $\omega = 0$; spectral functions are obtained by forward Fourier transform $A(\omega, t) = -\frac{1}{\pi} \text{Im} \int ds G^R(t+s, t) e^{i\omega s}$ for $t < 15$ and by backward Fourier transform for $t > 15$ (dashed vertical line at $t = 15$).

A possible scenario to explain the different behaviors would be that the back-action between electrons and phonons in the electron-boson problem can efficiently mitigate heating effects that arise from the interaction quench, and which would otherwise counteract the metallization. However, this is not the case here: in a solid, heating is compensated by a dissipative environment, which we have taken into account via the Ohmic heat bath (see methods). An effective temperature $1/\beta_{\text{eff}}$ obtained from a fit of the equilibrium fluctuation relation $A^<(\omega, t) = A(\omega, t)/(1 + e^{\beta_{\text{eff}}\omega})$ to the occupation functions $A^<(\omega, t)$ close to $\omega = 0$ at the latest time yields an even lower effective temperature for the $U_{\langle X^2 \rangle}$ -driven case ($\beta_{\text{eff}} \sim 9.5$) compared to the phonon driven case ($\beta_{\text{eff}} \sim 6.2$), see continuous red lines and dotted cyan lines in Figs. 4g and i. Moreover, $1/\beta_{\text{eff}}$ can characterize at most the low-energy quasi-particles, while the global state of the dynamic Hubbard model is a highly non-thermal driven state. The total energy at $t = 30$ is that of a system at inverse temperature $\beta \sim 2.083$ (spectrum shown by the dashed green line in Fig. 4g), and $\langle X \rangle$ is still oscillating (Fig. 2a). We therefore conclude that a time-dependent interaction $U_{\langle X^2 \rangle}$ or $U_{\langle X \rangle}^2$

plus phonon cooling cannot describe the enhancement of metallicity in the dynamic Hubbard model, but instead the driven nature of the state is essential. A possible explanation is that in addition to the static renormalization of U through $\langle X^2 \rangle$, there is a dynamic contribution via virtual phonon emission and absorption. Such induced interactions go as g^2/ω_{ph} in the anti-adiabatic phonon regime. In the presence of the X^2 -nonlinearity, an oscillating phonon may act similar to a dynamically modulated electron-phonon coupling, which allows for interactions mediated via phonon-Floquet sidebands, with an energy denominator $1/(\omega_{\text{ph}} \pm \Omega)$. Thus, such interactions can be strongly renormalized, in particular close to resonance $\omega_{\text{ph}} = \Omega$. While the present parameter regime, close to the IMT and with not too well-separated energy scales between ω_{ph} and bandwidth, makes an analytic understanding difficult, the numerical results in Fig. 3 unambiguously demonstrate substantial enhancement of the quasi-particle peak around the resonance. Another effect could be driving-induced undressing of polarons [40–42], but as we have concluded above, polaronic effects are probably not significant here.

Conclusions - In this study, we have analyzed a

generalized dynamic Hubbard model nonlinearly coupled to local phonons, relevant for the description of molecular solids, which is excited by an ultrafast pulse of local molecular vibration. By exactly treating the quantum phononic fluctuations, we show numerical evidence for the vibrationally-induced emergence of a quasi-particle peak in the electronic spectral function at $\omega \sim 0$, signalling the occurrence of an IMT. This observation should be relevant for the understanding of photo-induced superconductivity in molecular solids [25]. More

generally, the striking difference of our results to a simplified semiclassical treatment for the phonons imply the need for careful analysis of quantum phonon effects in the nonlinear phononics control of electronic properties.

F.G. would like to thank Nagamalleswararao Dasari for the useful discussions about the Ohmic bath. We were supported by the ERC starting grant No. 716648. The authors gratefully acknowledge the computational resources and support provided by the Erlangen Regional Computing Center (RRZE).

-
- [1] M. Först, C. Manzoni, S. Kaiser, Y. Tomioka, Y. Tokura, R. Merlin, and A. Cavalleri, “Nonlinear phononics as an ultrafast route to lattice control,” *Nature Physics* **7**, 854–856 (2011).
- [2] Alaska Subedi, Andrea Cavalleri, and Antoine Georges, “Theory of nonlinear phononics for coherent light control of solids,” *Phys. Rev. B* **89**, 220301 (2014).
- [3] D. N. Basov, R. D. Averitt, and D. Hsieh, “Towards properties on demand in quantum materials,” *Nature Materials* **16**, 1077–1088 (2017).
- [4] Matteo Rini, Ra’anan Tobey, Nicky Dean, Jiro Itatani, Yasuhide Tomioka, Yoshinori Tokura, Robert W Schoenlein, and Andrea Cavalleri, “Control of the electronic phase of a manganite by mode-selective vibrational excitation,” *Nature* **449**, 72–74 (2007).
- [5] A. D. Caviglia, R. Scherwitzl, P. Popovich, W. Hu, H. Bromberger, R. Singla, M. Mitrano, M. C. Hoffmann, S. Kaiser, P. Zubko, S. Gariglio, J.-M. Triscone, M. Först, and A. Cavalleri, “Ultrafast strain engineering in complex oxide heterostructures,” *Phys. Rev. Lett.* **108**, 136801 (2012).
- [6] R. Mankowsky, A. Subedi, M. Först, S. O. Mariager, M. Chollet, H. T. Lemke, J. S. Robinson, J. M. Glownia, M. P. Minitti, A. Frano, M. Fechner, N. A. Spaldin, T. Loew, B. Keimer, A. Georges, and A. Cavalleri, “Non-linear lattice dynamics as a basis for enhanced superconductivity in $\text{YBa}_2\text{Cu}_3\text{O}_{6.5}$,” *Nature* **7529**, 71–73 (2014).
- [7] M. Först, R. I. Tobey, S. Wall, H. Bromberger, V. Khanna, A. L. Cavalieri, Y.-D. Chuang, W. S. Lee, R. Moore, W. F. Schlotter, J. J. Turner, O. Krupin, M. Trigo, H. Zheng, J. F. Mitchell, S. S. Dhesi, J. P. Hill, and A. Cavalleri, “Driving magnetic order in a manganite by ultrafast lattice excitation,” *Phys. Rev. B* **84**, 241104 (2011).
- [8] M. Först, A. D. Caviglia, R. Scherwitzl, R. Mankowsky, P. Zubko, V. Khanna, H. Bromberger, S. B. Wilkins, Y.-D. Chuang, W. S. Lee, W. F. Schlotter, J. J. Turner, G. L. Dakovski, M. P. Minitti, J. Robinson, S. R. Clark, D. Jakob, J.-M. Triscone, J. P. Hill, S. S. Dhesi, and A. Cavalleri, “Spatially resolved ultrafast magnetic dynamics initiated at a complex oxide heterointerface,” *Nature Materials* **14**, 883–888 (2015).
- [9] T. F. Nova, A. Cartella, A. Cantaluppi, M. Först, D. Bossini, R. V. Mikhaylovskiy, A. V. Kimel, R. Merlin, and A. Cavalleri, “An effective magnetic field from optically driven phonons,” *Nature Physics* **2**, 132–136 (2017).
- [10] E. Pomarico, M. Mitrano, H. Bromberger, M. A. Sentef, A. Al-Temimi, C. Coletti, A. Stöhr, S. Link, U. Starke, C. Cacho, R. Chapman, E. Springate, A. Cavalleri, and I. Gierz, “Enhanced electron-phonon coupling in graphene with periodically distorted lattice,” *Phys. Rev. B* **95**, 024304 (2017).
- [11] R. Singla, G. Cotugno, S. Kaiser, M. Först, M. Mitrano, H. Y. Liu, A. Cartella, C. Manzoni, H. Okamoto, T. Hasegawa, S. R. Clark, D. Jakob, and A. Cavalleri, “Thz-frequency modulation of the hubbard u in an organic mott insulator,” *Phys. Rev. Lett.* **115**, 187401 (2015).
- [12] Dante M. Kennes, Eli Y. Wilner, David R. Reichman, and Andrew J. Millis, “Transient superconductivity from electronic squeezing of optically pumped phonons,” *Nature Physics* **13**, 479–483 (2017).
- [13] M. A. Sentef, “Light-enhanced electron-phonon coupling from nonlinear electron-phonon coupling,” *Phys. Rev. B* **95**, 205111 (2017).
- [14] Alexandre Marciniak, Stefano Marcantoni, Francesca Giusti, Filippo Glerean, Giorgia Sparapassi, Tobia Nova, Andrea Cartella, Simone Latini, Francesco Valiera, Angel Rubio, Jeroen van den Brink, Fabio Benatti, and Daniele Fausti, “Vibrational coherent control of localized d-d electronic excitation,” arXiv e-prints , arXiv:2003.13447 (2020), arXiv:2003.13447 [cond-mat.mtrl-sci].
- [15] M. Puviani and M. A. Sentef, “Quantum nonlinear phononics route towards nonequilibrium materials engineering: Melting dynamics of a ferrielectric charge density wave,” *Phys. Rev. B* **98**, 165138 (2018).
- [16] Michael Lang and Jens Müller, “Organic superconductors,” in *The Physics of Superconductors: Vol. II. Superconductivity in Nanostructures, High-Tc and Novel Superconductors, Organic Superconductors*, edited by K. H. Bennemann and J. B. Ketterson (Springer Berlin Heidelberg, Berlin, Heidelberg, 2004) pp. 453–554.
- [17] Arzhang Ardavan, Stuart Brown, Seiichi Kagoshima, Kazushi Kanoda, Kazuhiko Kuroki, Hatsumi Mori, Masao Ogata, Shinya Uji, and Jochen Wosnitza, “Recent topics of organic superconductors,” *Journal of the Physical Society of Japan* **81**, 011004 (2012).
- [18] H. Okamoto, H. Matsuzaki, T. Wakabayashi, Y. Takahashi, and T. Hasegawa, “Photoinduced metallic state mediated by spin-charge separation in a one-dimensional organic mott insulator,” *Phys. Rev. Lett.* **98**, 037401 (2007).
- [19] M. Mitrano, G. Cotugno, S. R. Clark, R. Singla, S. Kaiser, J. Stähler, R. Beyer, M. Dressel, L. Baldassarre, D. Nicoletti, A. Perucchi, T. Hasegawa, H. Okamoto, D. Jakob, and A. Cavalleri, “Pressure-dependent relaxation in the photoexcited mott insulator ET-F₂TCNQ: Influence of hopping and correlations on

- quasiparticle recombination rates," *Phys. Rev. Lett.* **112**, 117801 (2014).
- [20] S. Kaiser, S. R. Clark, D. Nicoletti, G. Cotugno, R. I. Tobey, N. Dean, S. Lupi, H. Okamoto, T. Hasegawa, D. Jaksch, and A. Cavalleri, "Optical properties of a vibrationally modulated solid state mott insulator," *Scientific Reports* **4**, 5556 (2014).
- [21] Massimo Capone, Michele Fabrizio, Claudio Castellani, and Erio Tosatti, "Colloquium: Modeling the unconventional superconducting properties of expanded A_3C_{60} fullerides," *Rev. Mod. Phys.* **81**, 943–958 (2009).
- [22] M. Mitrano, A. Cantaluppi, D. Nicoletti, S. Kaiser, A. Perucchi, S. Lupi, P. Di Pietro, D. Pontiroli, M. Riccò, S. R. Clark, D. Jaksch, and A. Cavalleri, "Possible light-induced superconductivity in k_3C_{60} at high temperature," *Nature* **591**, 461–464 (2016).
- [23] A. Cantaluppi, M. Buzzi, G. Jotzu, D. Nicoletti, M. Mitrano, D. Pontiroli, M. Riccò, A. Perucchi, P. Di Pietro, and A. Cavalleri, "Pressure tuning of light-induced superconductivity in k_3C_{60} ," *Nature Physics* **8**, 837–841 (2018).
- [24] M. Budden, T. Gebert, M. Buzzi, G. Jotzu, E. Wang, T. Matsuyama, G. Meier, Y. Laplace, D. Pontiroli, M. Riccò, F. Schlawin, D. Jaksch, and A. Cavalleri, "Evidence for metastable photo-induced superconductivity in K_3C_{60} ," arXiv e-prints , arXiv:2002.12835 (2020), arXiv:2002.12835 [cond-mat.supr-con].
- [25] M. Buzzi, D. Nicoletti, M. Fechner, N. Tancogne-Dejean, M. A. Sentef, A. Georges, M. Dressel, A. Henderson, T. Siegrist, J. A. Schlueter, K. Miyagawa, K. Kanoda, M. S. Nam, A. Ardavan, J. Coulthard, J. Tindall, F. Schlawin, D. Jaksch, and A. Cavalleri, "Photomolecular high temperature superconductivity," (2020), arXiv:2001.05389 [cond-mat.supr-con].
- [26] Y. Kawakami, S. Iwai, T. Fukatsu, M. Miura, N. Yoneyama, T. Sasaki, and N. Kobayashi, "Optical modulation of effective on-site coulomb energy for the mott transition in an organic dimer insulator," *Phys. Rev. Lett.* **103**, 066403 (2009).
- [27] P. Pincus, "Polaron effects in the nearly atomic limit of the hubbard model," *Solid State Communications* **11**, 51 – 54 (1972).
- [28] J. E. Hirsch, "Dynamic hubbard model," *Phys. Rev. Lett.* **87**, 206402 (2001).
- [29] K. Itoh, H. Itoh, M. Naka, S. Saito, I. Hosako, N. Yoneyama, S. Ishihara, T. Sasaki, and S. Iwai, "Collective excitation of an electric dipole on a molecular dimer in an organic dimer-mott insulator," *Phys. Rev. Lett.* **110**, 106401 (2013).
- [30] Daniel Neuhauser, Tae-Jun Park, and Jeffrey I. Zink, "Analytical derivation of interference dips in molecular absorption spectra: Molecular properties and relationships to fano's antiresonance," *Phys. Rev. Lett.* **85**, 5304–5307 (2000).
- [31] J. E. Hirsch, "Electron-hole asymmetry is the key to superconductivity," *International Journal of Modern Physics B* **17**, 3236–3241 (2003).
- [32] Hideo Aoki, Naoto Tsuji, Martin Eckstein, Marcus Kollar, Takashi Oka, and Philipp Werner, "Nonequilibrium dynamical mean-field theory and its applications," *Reviews of Modern Physics* **86**, 779–837 (2014).
- [33] Martin Eckstein and Philipp Werner, "Nonequilibrium dynamical mean-field calculations based on the noncrossing approximation and its generalizations," *Phys. Rev. B* **82**, 115115 (2010).
- [34] Hugo U. R. Strand, Martin Eckstein, and Philipp Werner, "Nonequilibrium dynamical mean-field theory for bosonic lattice models," *Phys. Rev. X* **5**, 011038 (2015).
- [35] Philipp Werner and Martin Eckstein, "Phonon-enhanced relaxation and excitation in the holstein-hubbard model," *Phys. Rev. B* **88**, 165108 (2013).
- [36] Philipp Werner and Martin Eckstein, "Effective doublon and hole temperatures in the photo-doped dynamic hubbard model," *Structural Dynamics* **3**, 023603 (2016), <https://doi.org/10.1063/1.4935245>.
- [37] Hsing-Ta Chen, Guy Cohen, Andrew J. Millis, and David R. Reichman, "Anderson-holstein model in two flavors of the noncrossing approximation," *Phys. Rev. B* **93**, 174309 (2016).
- [38] Martin Eckstein and Philipp Werner, "Photoinduced States in a Mott Insulator," *Physical Review Letters* **110**, 126401 (2013).
- [39] Francesco Peronaci, Olivier Parcollet, and Marco Schiró, "Enhancement of local pairing correlations in periodically driven mott insulators," *Phys. Rev. B* **101**, 161101 (2020).
- [40] J. E. Hirsch, "Quasiparticle undressing in a dynamic hubbard model: Exact diagonalization study," *Phys. Rev. B* **66**, 064507 (2002).
- [41] J. E. Hirsch, "Polaronic superconductivity in the absence of electron-hole symmetry," *Phys. Rev. B* **47**, 5351–5358 (1993).
- [42] P. Gaal, W. Kuehn, K. Reimann, M. Woerner, T. El-saesser, and R. Hey, "Internal motions of a quasiparticle governing its ultrafast nonlinear response," *Nature* **450**, 1210–1213 (2007).